

A Time Optimal Reactive Collision Avoidance Method for UAVs Based on a Modified Collision Cone Approach

Manaram Gnanasekera¹ and Jay Katupitiya¹

Abstract—UAVs or Unmanned Aerial Vehicles are an upcoming technology which has eased human lifestyles in many ways. Due to this trend future skies have a risk of getting congested. In such a situation time optimal collision avoidance would be extremely vital to travel in a shortest possible time by avoiding collisions. The paper proposes a novel method for time optimal collision avoidance for UAVs. The proposed algorithm is constructed as a three-stage approach based on the Collision Cone method with slight modifications. A sliding mode controller is used as the control law for the navigation. Mathematical proofs are included to verify the time optimality of the proposed method. The efficiency and the applicability of the work carried out is confirmed by both simulation and experimental results. An automated Matrice 600 Pro hexacopter has been used for the experiments.

I. INTRODUCTION

Day by day UAVs (Unmanned Aerial Vehicles) become commercialized in an unbelievable pace. With the commercialization of aerial vehicles, the usage of UAVs will increase rapidly in future. More and more UAVs, will lead to congestion. Similar to road accidents, UAV congestion will give rise to aerial collisions. As UAVs carry flammable materials, collisions could lead to disastrous situations. Therefore, collision avoidance has become salient in UAV based applications.

The collision avoidance literature could be categorized as path planning based on global information, and reactive collision avoidance based on local information [1]. Mobile robots which are programmed with the global method will require information about the entire environment in a form of a map, whereas reactive methods will be focussed on a particular area in an environment. As examples, methods such as A* [2], D* [3] and D* Lite [4] and Probabilistic Road Maps (PRM) [5] could be shown as global methods. However, due to the high computational cost [1], global methods are not vastly used in complex changing environments. Since reactive methods are focused on local information they are robust to rapid environmental changes and posses low computational costs. Some versions of RRT [6], Artificial Potential Fields (APF) [7] and velocity obstacle/collision cone [8] methods are examples for reactive methods. Despite the fine remarks, RRT methods hold a high computational cost and Artificial Potential Fields has the potential to get trapped at local minima [9]. Collision cone on the other hand has the ability to predict a collision before hand compared

to many other reactive methods. This particular quality has made the authors of this paper to leverage the collision cone to be at the core of the proposed work.

The concept of collision cone has many variants. The collision cone was first believed to be proposed in [10]. With slight variations the method of velocity obstacle was first introduced in [8]. Another variant in the name of Clear Path was proposed in [11] to handle dense scenarios incorporating mass number of agents based on discrete optimization. The method in [12] assumes all the agents have the same shape and same algorithm and hence build a velocity obstacle for collision information sharing. The authors of [13] have generalised the velocity obstacle concept for a car like-robot to formulate controls which will lead to future collisions.

Despite the large volume available, the collision cone concept or any of its variants haven't made a noticeable contribution over time optimal collision avoidance. Time becomes a vital constraint in most of the mobile robot applications such as delivery, search and rescue, military etc. Out of the limited literature, authors of [14] have presented a collision cone based method for trajectory optimization. The method comprise non-linear time scaling techniques [15] to vary the travelling velocity of the robot to avoid collisions in a reactive manner [16]. A notable feature of the method is that it remains on the travelling path and not a single heading change is made by the mobile robot. Furthermore, this method is robust to obstacle movement uncertainties. Even though, the method in [14] addresses the time optimality problem it will not be able to avoid static obstacles and obstacles moving directly towards the robot.

The authors of this paper modify the collision cone method to reactively avoid all obstacles ensuring time optimality. The proposed method allows heading variation while maintaining the speed at a constant value. Therefore, the mobile robot has the ability to avoid both static and dynamic obstacles. The validity of the proposed algorithm has been proven through both simulation and experimental results along with rigorous mathematical proofs.

The organization of the content is as follows. Section II provides the problem description and mathematical proof of the theorem. The single obstacle problem is discussed in section III and the multiple obstacle problem is discussed in section IV. Section V includes simulation and experimental results. Section VI concludes the paper with few final remarks.

¹The authors are with the of Mechanical and Manufacturing Engineering, University of New South Wales, Sydney, Australia
m.gnanasekera@unsw.edu.au,
j.katupitiya@unsw.edu.au

II. PROBLEM DESCRIPTION

We consider an under actuated UAV which travels along a planer surface W , $W \subset \mathbb{R}^2$ by being at a constant height from the ground. We assume the UAV to be a planer circle with radius R_u . The position of the UAV could be given by (x_u, y_u) . Let the maximum speed of the UAV be v_u ($v_u > 0$). Let $\theta_u(t)$ ($[-\pi, \pi]$) be the variable heading angle with respect to the x axis. As the proposed method has a heading based strategy and fixed speed, the rotational and the translational motion could be introduced as in (1). I is the inertia of the UAV and B is a resistance constant. The term $(-B/I)\omega_u(t)$ is the Rotational Coulomb resistance component of the UAV.

$$\begin{aligned}\dot{x}_u(t) &= v_u \cos(\theta_u(t)) \\ \dot{y}_u(t) &= v_u \sin(\theta_u(t)) \\ \dot{\theta}_u(t) &= \omega_u(t) \\ \ddot{\omega}_u(t) &= (-B/I)\omega_u(t) + \tau/I\end{aligned}\quad (1)$$

Due to the heading based navigational strategy the difference between the calculated heading by the proposed algorithm ($\theta_a(t)$) and the current heading ($\theta_u(t)$) could be taken as the error (2).

$$e(t) = \theta_a(t) - \theta_u(t) \quad (2)$$

We consider the following navigation law (3).

$$\tau = \text{sgn}(e(t)) \quad (3)$$

where,

$$\text{sgn}(e(t)) = \begin{cases} -1 & \text{if } e(t) < 0, \\ 0 & \text{if } e(t) = 0, \\ 1 & \text{if } e(t) > 0. \end{cases} \quad (4)$$

The purpose of the UAV is to travel to a target located at (x_G, y_G) by avoiding disjoint obstacles $\cup_{i=1}^n O_i$ ($\forall O_i \subset W$). We first consider a single obstacle situation as in Fig. 2. The task of the UAV is to travel from S to G .

Theorem 1: Consider the UAV to be at S and the goal position to be at G (Fig. 2). $O(t)$ is a moving obstacle ($\forall t, O(t) \subset W$). $A(t)$ and $B(t)$ are two points on the periphery of the obstacle (Fig. 2). At $t = t_A$, $SA(t_A)$ becomes a tangent to the obstacle $O(t_A)$. At $t = t_B$, $B(t_B)G$ becomes a tangent to the obstacle $O(t_B)$. If $\overline{A(t_A)B(t_B)}$ is a path of a point moving on the periphery of the obstacle from $A(t_A)$ to $B(t_B)$, $SA(t_A)B(t_B)G$ is the time optimal collision free path.

Proof of Theorem 1: Let $l(t)$ be the straight line connecting the UAV's current location and the goal's location, ϕ be the angle between $l(t)$ and the velocity vector $\vec{v}_u(t)$. If the UAV is travelling at the maximum speed v_u , (5) becomes the cost function and should be minimized to travel to the goal's position. Let T_S be the time when the UAV reaches S and T_G be the UAV's goal reaching time.

$$J(t) = \int_{T_S}^{T_G} v_u \sin(\phi) dt \quad (5)$$

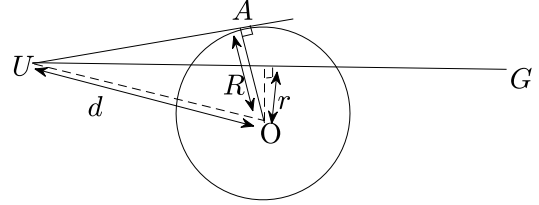


Fig. 1: The diagram shows a moment of the collision situation which pictorially explains $\angle AUO$ and $\angle GUO$.

If $\angle AUO$ is θ and $\angle GUO$ is α (as shown in Fig. 1), the collision constraint could be introduced as (6). If a certain ϕ angle is collision free, $G(\phi) = 0$. Where, $0 \leq \phi \leq \frac{\pi}{2}$.

$$G(\phi) = \max [(\theta - \alpha) - \phi, 0] \quad (6)$$

According to (6) the collision free ϕ angles are $\theta - \alpha \leq \phi \leq \frac{\pi}{2}$. At a given $t = T$ time the minimum cost value will be given when $\phi = \theta - \alpha$. Therefore, the total minimum cost could be given as in (7).

$$J_{min}(t) = \int_{T_S}^{T_G} v_u \sin(\theta - \alpha) dt \quad (7)$$

According to Fig. 2, if (7) is satisfied, after $t = t_A$ the UAV should reach $A(t_A)$. $SA(t_A)$ should be a tangent to $O(t_A)$. Thereafter, the UAV needs to travel on a moving periphery until the line of sight towards the goal becomes clear. After $t = t_B$, if the line of sight becomes clear at point $B(t_B)$, $B(t_B)G$ should be a tangent to $O(t_B)$.

This completes the proof of Theorem 1.

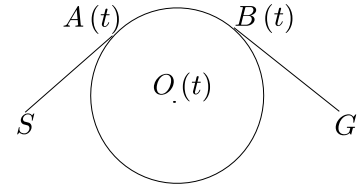


Fig. 2: The summary of the optimal path which the UAV should travel to avoid the collision. The UAV should start from S and reach the periphery at $A(t)$ and move along the moving periphery to reach $B(t)$. Navigate straight to G from $B(t)$.

III. SINGLE OBSTACLE PROBLEM

First, the problem will be divided into three parts as hazard stage, intermediate stage and post hazard stage for ease of discussion. At the hazard stage the UAV senses the obstacle and avoids the potential collision in the most time optimal manner and then reaches the posterior safety boundary (Fig. 3) of the obstacle (reaches the point $A(t)$ at a given time $t = t_A$). The straight travel path of the UAV from $A(t_A)$ to G is infeasible due to the obstacle. Therefore, during the intermediate stage the UAV travels in a time optimal collision free manner till the line of sight

between the UAV and the goal becomes clear. At the post hazard stage the UAV has already avoided the collision and has to find the time optimal path to the goal.

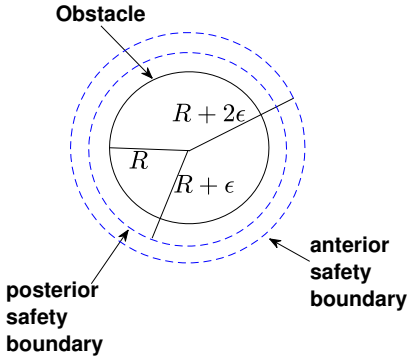


Fig. 3: Safety boundaries of the obstacle. Obstacle has a radius R , the posterior safety boundary has a radius of $R + \epsilon$ and the anterior safety boundary has a radius of $R + 2\epsilon$.

A. Hazard Stage

As described in the Introduction a collision cone [10] based approach with modifications to find the optimum heading, will be used for the collision avoidance. Fig. 4 shows a typical collision situation represented in the form of a collision cone. The collision cone is drawn with respect to the UAV. At the hazard stage the distance between the UAV and the obstacle is given as d . As in Fig. 4 the two tangents from the obstacle's position to the UAV's posterior safety boundary could be taken as P_1 and P_2 . Let γ be the angle $\angle UOP_2$ and ψ be the angle between OU and the relative vector \vec{v}_{ou} .

Definition 1: We can predict a future collision situation when the condition $\psi < \gamma$ is satisfied.

In order to avoid the collision a heading change which satisfies $\psi > \gamma$ should be made by the UAV. There will be many \vec{v}_{ou} vectors which would satisfy the condition $\psi > \gamma$, however, the most optimum vector according to Theorem 1 would be the vector pointing at point P_2 . In other word this vector should coincide with OP_2 line. Therefore, the heading of the UAV should be changed as if the vector \vec{v}_{ou} coincides with OP_2 edge all the time.

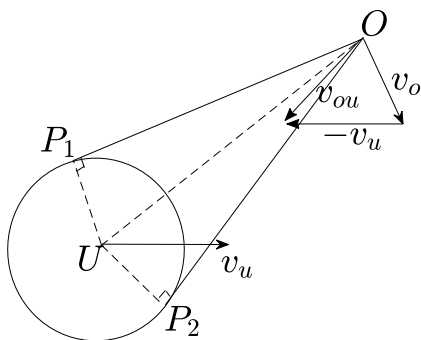


Fig. 4: Collision Cone drawn with respect to the UAV velocity v_u .

Let α be the angle between OP_2 and the obstacle's velocity vector \vec{v}_o . If \vec{v}_{ou} comes on top of OP_2 (pointing at P_2), the angle between \vec{v}_{ou} and \vec{v}_o becomes α .

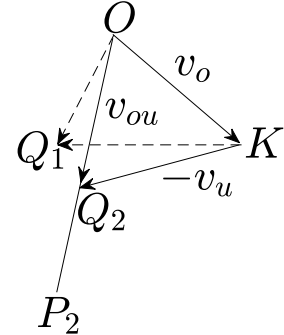


Fig. 5: $O\vec{Q}_1$ is the relative velocity vector before the heading correction. $K\vec{Q}_1$ is the negated velocity vector of the UAV before the heading correction. $O\vec{Q}_2$ is the relative velocity vector after the heading correction. $K\vec{Q}_2$ is the negated velocity vector after heading correction.

Fig. 5 shows the vector diagram which consists the headings of \vec{v}_{ou} and \vec{v}_u before and after the UAV's heading correction. The vectors point at Q_1 before the heading correction and point at Q_2 after the heading correction.

Let λ be the angle $\angle OKQ_1$. Furthermore, let μ be the angle $\angle OQ_2K$. By applying the "Sine Law" the value of μ could be obtained as $\arcsin\left(\frac{v_o}{v_u} \sin(\alpha)\right)$. Let β be the angle $\angle OKQ_2$ and the value of β could be given as $(\pi - (\alpha + \mu))$. Therefore, the heading correction ($\angle Q_1KQ_2$) could be given as in equation (8).

$$\theta_a(t) - \theta_u(t) = \beta - \lambda \quad (8)$$

where, the solution of (8) could be applied directly to (2).

B. Intermediate Stage

If the UAV is at $A(t_A)$, when $t = t_A$ (Fig. 2). According to Theorem 1 the UAV should travel over the posterior safety boundary and reach $B(t_B)$, when $t = t_B$. Point $A(t_A)$ is the last stage of the hazard stage which becomes a tangent point to the circular obstacle. According to Fig. 2 it is obvious that the UAV cannot travel in a straight line and reach the goal position G . We introduce an algorithm to manoeuvre the UAV during the intermediate stage.

If the UAV is at $(x_u(t), y_u(t))$ and the heading is $\theta_u(t)$, we will predict the position of the UAV at the next δt sample time when $\theta_u(t + \delta t) = \theta_u(t)$, $\theta_u(t + \delta t) = \theta_u(t) + \delta\theta$ and $\theta_u(t + \delta t) = \theta_u(t) - \delta\theta$. Where $\delta\theta \in \mathbb{R}$.

$$\begin{aligned} \hat{x}_{u1} &= x_u(t) + v_u \cos(\theta_u - \delta\theta)\delta t \\ \hat{y}_{u1} &= y_u(t) + v_u \sin(\theta_u - \delta\theta)\delta t \end{aligned} \quad (9)$$

$$\begin{aligned} \hat{x}_{u2} &= x_u(t) + v_u \cos(\theta_u)\delta t \\ \hat{y}_{u2} &= y_u(t) + v_u \sin(\theta_u)\delta t \end{aligned} \quad (10)$$

$$\begin{aligned} \hat{x}_{u3} &= x_u(t) + v_u \cos(\theta_u + \delta\theta)\delta t \\ \hat{y}_{u3} &= y_u(t) + v_u \sin(\theta_u + \delta\theta)\delta t \end{aligned} \quad (11)$$

We assume the obstacle to have a fixed heading θ_o . If the obstacle is at $(x_o(t), y_o(t))$, we also predict the position of the obstacle at $t = t + \delta t$.

$$\begin{aligned}\hat{x}_o &= x_o(t) + v_o \cos(\theta_o)\delta t \\ \hat{y}_o &= y_o(t) + v_o \sin(\theta_o)\delta t\end{aligned}\quad (12)$$

We calculate R_1 as in (13), R_2 as in (14) and R_3 as in (15). The intent of the UAV during the intermediate stage is to be between the anterior safety boundary (Fig. 3) and the obstacle (Fig. 3). In order to satisfy this condition we first calculate δR_1 , δR_2 and δR_3 in (16), (17) and (18). The radius of the obstacle is R .

$$R_1 = \sqrt{(\hat{x}_{u1} - \hat{x}_o)^2 + (\hat{y}_{u1} - \hat{y}_o)^2} \quad (13)$$

$$R_2 = \sqrt{(\hat{x}_{u2} - \hat{x}_o)^2 + (\hat{y}_{u2} - \hat{y}_o)^2} \quad (14)$$

$$R_3 = \sqrt{(\hat{x}_{u3} - \hat{x}_o)^2 + (\hat{y}_{u3} - \hat{y}_o)^2} \quad (15)$$

$$\delta R_1 = |(R_1 - R)| \quad (16)$$

$$\delta R_2 = |(R_2 - R)| \quad (17)$$

$$\delta R_3 = |(R_3 - R)| \quad (18)$$

We apply the results of (16),(17) and (18) in Algorithm 1 to find the optimum heading which would keep the UAV between the two aforementioned boundaries.

Algorithm 1 Calculating the optimum heading

```

Input:  $\delta R_1$ ,  $\delta R_2$ ,  $\delta R_3$ 
Output:  $\theta(t + \delta t)$ 
1: if  $(\delta R_1 < \delta R_2)$ and $(\delta R_1 < \delta R_3)$  then
2:    $\theta(t + \delta t) \leftarrow \theta(t) - \delta\theta$ 
3: else if  $(\delta R_2 < \delta R_1)$ and $(\delta R_2 < \delta R_3)$  then
4:    $\theta(t + \delta t) \leftarrow \theta(t)$ 
5: else
6:    $\theta(t + \delta t) \leftarrow \theta(t) + \delta\theta$ 
7: end if
```

C. Post hazard Stage

During the post hazard stage the UAV will be travelling directly to the goal from $B(t_B)$ on a straight line. Finding the point $B(t_B)$ is straightforward. The $B(t_B)G$ line should not be intercepting the circle which has a radius of R_B (19). In fact $B(t_B)G$ should be a tangent to this circle. It should be noted that the value of R_B should be $R \leq R_B \leq R + 2\epsilon$. The UAV will be at point $B(t_B)$ at $t = t_B$.

$$R_B = \sqrt{(x_u(t_B) - x_o(t_B))^2 + (y_u(t_B) - y_o(t_B))^2} \quad (19)$$

IV. MULTIPLE OBSTACLE PROBLEM

A typical multiple obstacle situation is shown in Fig. 6. The UAV labelled as U travels towards the goal position G . A potential collision has been detected with two obstacles O_1 and O_2 . Let R_u be the radius of the UAV, r_1 be the radius of O_1 and r_2 be the radius of O_2 . If $r_1 > r_2$, the UAV's radius will be taken as $R_u + r_1$ when drawing the collision cone. In a multiple collision scenario collision cones should be drawn for all the obstacles. The difference between the multiple obstacle scenario and the single obstacle scenario is the hazard stage. The other two stages remain similar. It is important to note that the v_{ou} vector in Fig. 4 could be directed at OP_1 direction or OP_2 direction. However, in a single obstacle scenario the relative velocity vector could only be directed at one direction unless the vector is right on OU . The main reason behind this selection is the cost function (5). The angle between v_{ou} and OP_2 is much smaller than that of v_{ou} and OP_1 . The smaller angle will result a low cost value according to (7). However this selection criteria will not be valid to a multiple collision situation. Therefore, heading change of the relative velocity vector in both clockwise and anticlockwise directions should be considered in a multiple collision scenario. As an example v_{o1u} vector could be directed towards the direction of O_1P_2 or O_1P_1 . In other words one is a clockwise correction and the other is an anticlockwise correction. Let β_{oi} become the anticlockwise correction angle, where $\{oi|o1, \dots, on\}$ is the obstacle. Similarly, α_{oi} become the clockwise correction. Lets consider a scenario with n number of obstacles. We introduce a three step process to find the value of the correction angle and whether it should be clockwise or anticlockwise. According to (20), the angle with the highest β_{oi} will be selected.

$$\max \{\beta_{o1}, \dots, \beta_{on}\} = \eta_\beta \quad (20)$$

Similarly, the angle with the highest α_{oi} will be selected (21).

$$\max \{\alpha_{o1}, \dots, \alpha_{on}\} = \eta_\alpha \quad (21)$$

Then the minimum value between η_β and η_α will be selected.

$$\min \{\eta_\alpha, \eta_\beta\} = \eta \quad (22)$$

η becomes the $\angle P_2 OQ_1$ angle in Fig.5. From here on, the problem could be considered as a single obstacle problem and the η value could be used in the hazard stage for the heading calculation.

V. RESULTS AND DISCUSSION

The algorithm proposed in this paper was tested in simulation and experimentally. A Matlab based test bench was used for the simulations and a Matrice 600 Pro Hexacopter was used for the experiments. A distance of 200 m has been taken as the sensing distance during the simulations and in the experiments the distance has been considered as 5 m.

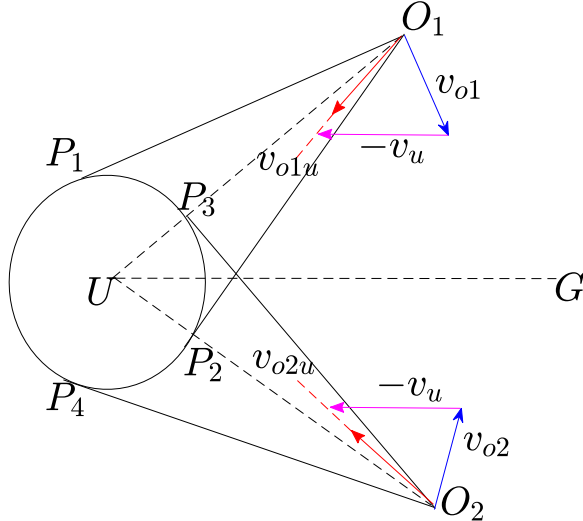


Fig. 6: Multiple Obstacle situation. The UAV U has sensed obstacle O_1 and obstacle O_2 on the way to G .

A. Computer Simulations

We consider a situation where the UAV travels at a speed of 5 ms^{-1} towards a static goal located at co-ordinates (300,300). We consider the UAV to have a unit radius (<https://youtu.be/bWmVXszXCS4>). While moving towards the goal, at a co-ordinate (175,175) the UAV senses an obstacle which will lead to a future collision. Fig. 7 shows the obstacle avoidance scenario along with the obstacle's travel path. The obstacle has a radius of 100 m, a speed of 4.8 ms^{-1} and a heading angle of $-2\pi/3 \text{ rad}$ with the x axis.

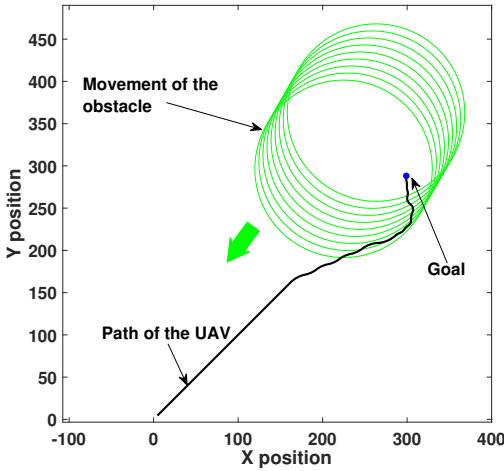


Fig. 7: Paths of the UAV and the obstacle in the single obstacle simulation.

The hazard stage of the first collision scenario is shown in Fig. 8. Following the detection of the obstacle at (175,175), the UAV has made an instant heading change according to (8). Thereafter, with the aid of (3) and (8) the UAV has

reached the posterior safety boundary of the obstacle. The actual boundary of the obstacle which has a radius of R , the posterior safety boundary which has a radius of $R + \epsilon$ and the anterior safety boundary with a radius of $R + 2\epsilon$ which will be used in the intermediate stage have been zoomed in in Fig. 8. The final position of the UAV during the hazard stage will be a tangent to the posterior safety boundary. However due to the sliding mode nature of the navigation law the closest point to the posterior boundary will be taken as the tangent point (point A according to Fig. 2).

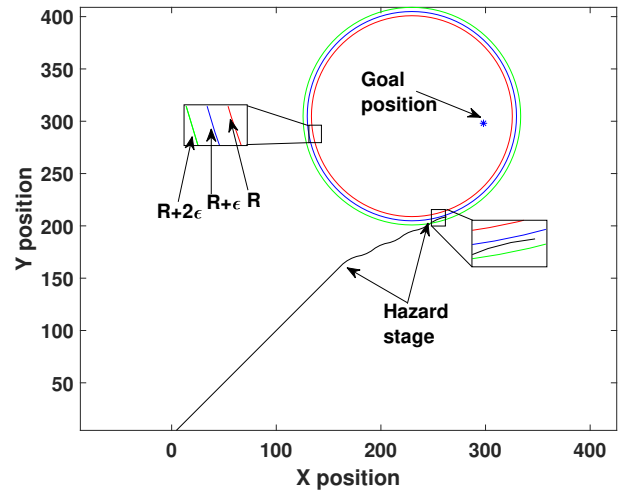


Fig. 8: Hazard stage of the single obstacle simulation.

A sample from the intermediate stage is shown in Fig. 9. The obstacle is marked as M and the anterior safety boundary is marked as N . During the intermediate stage of this scenario the UAV navigates between M and N with the aid of Algorithm 1.

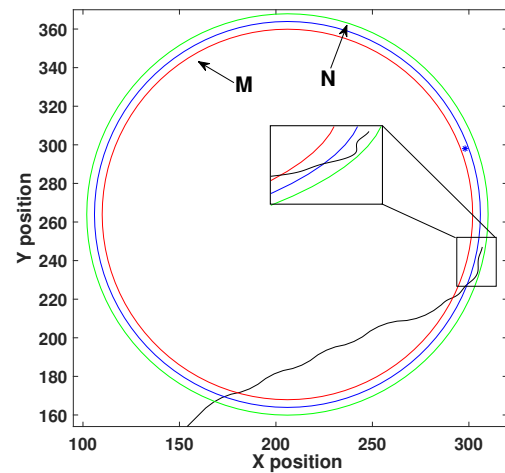


Fig. 9: Intermediate stage of the single obstacle simulation.

During the post hazard stage the navigation law (3)

navigates the UAV directly towards the goal as in Fig. 10. The results shown in Fig. 8, Fig. 9 and Fig. 10 confirms soundness of the method proposed in Section III.

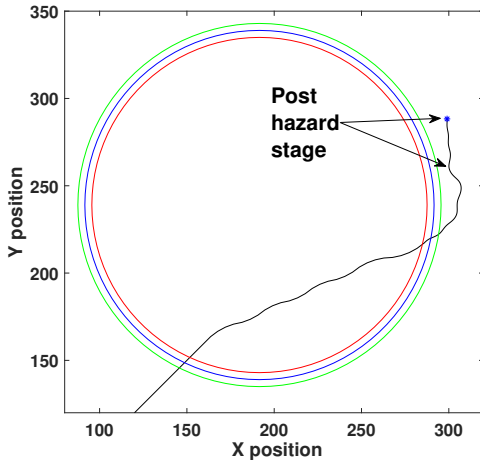


Fig. 10: Post hazard stage of the single obstacle simulation.

In Fig. 11 we have simulated the multiple collision scenario discussed in Section IV. Obstacle 1 travels at a speed of 4.8 ms^{-1} and at a heading angle of $-2\pi/3.3 \text{ rad}$. Another obstacle (Obstacle 2) travels towards the path of the UAV at a heading angle of $-\pi \text{ rad}$ and at a speed of 5 ms^{-1} . Both of the obstacles have 60 m radii. The UAV (which has a unit radius) in Fig. 11 has sensed two obstacles at around (202,202). According to the dotted line in Fig. 11 it is clear that the UAV collides with both obstacles if it had headed straight to the goal. Furthermore, Fig. 11 claims that the UAV requires a larger heading to avoid the Obstacle 1 compared to Obstacle 2. Therefore, the UAV has made the larger heading change to avoid both the obstacles. The complete travel paths of the UAV and the two obstacles are shown in Fig. 12. It should be noted that in most occasions the sensed obstacles have a high chance of colliding with each other in a multiple obstacle scenario.

B. Experimental Results

As single obstacle problem is the crux of the proposed methodology, we have tested the single obstacle problem by conducting two different experiments. It is important to mention that in the experiments the τ value in the control equation will be replaced by a constant heading value of 2 rad . As a result, the controller will be switching between -2 rad , $+2 \text{ rad}$ and 0 rad . In both experiments the obstacle is having a 2 m radius.

The hexacopter has travelled at 0.3 ms^{-1} speed in both cases. In the first experiment the hexacopter has started to travel towards a goal located at (11.6,-11.8). At a co-ordinate around (7,-7) the hexacopter has sensed an obstacle which travels in a direction of $\pi/2.1 \text{ rad}$ with a speed 0.2 ms^{-1} . Fig. 13 shows the complete travel path of the hexacopter and the obstacle. The hexacopter has reached the posterior safety

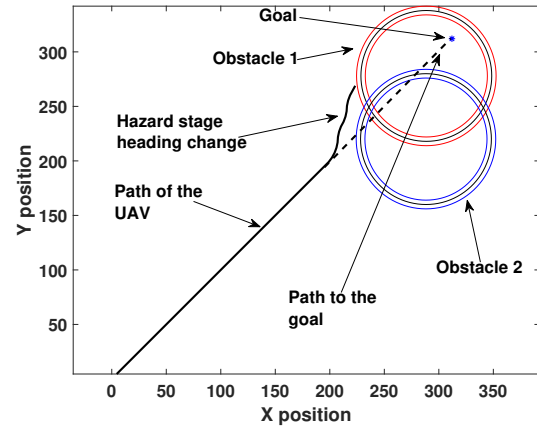


Fig. 11: Collision situation with multiple obstacles (Obstacle 1 and Obstacle 2).

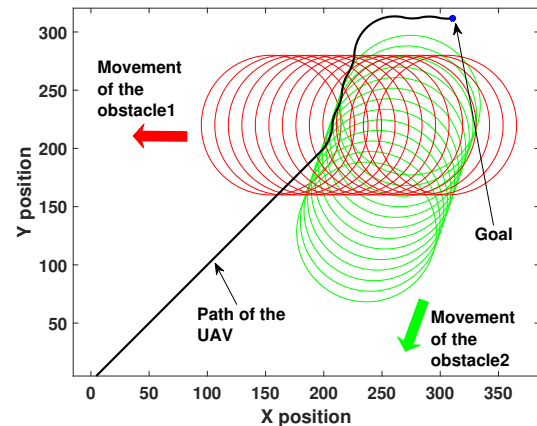


Fig. 12: Paths of the UAVs and the obstacles in the multiple obstacle simulation.

boundary successfully during the hazard stage according to Fig. 14.

It could be noted that at the last point of the hazard stage, the line of sight to the goal location has been blocked by the posterior safety boundary.

During the intermediate stage a $\delta\theta$ value of $\pi/16.0 \text{ rad}$ has been used for Algorithm 1. As shown in Fig. 15 the hexacopter has navigated between M and N boundaries until the goal position.

In the second experiment, the hexacopter travels towards a goal located at (14,14). At a co-ordinate around (7,7) the hexacopter has sensed an obstacle which travels in a speed 0.2 ms^{-1} at a direction of $-\pi/2.1 \text{ rad}$ (Fig. 16). As per Fig. 17 and Fig. 18 the hexacopter has successfully completed the hazard stage and hasn't moved away from the M and N boundaries during the intermediate stage. However, during the post hazard stage the hexacopter hasn't

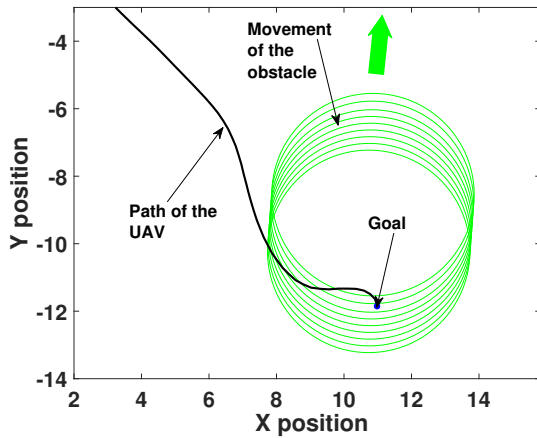


Fig. 13: Paths of the hexacopter and the obstacle in the first experiment.

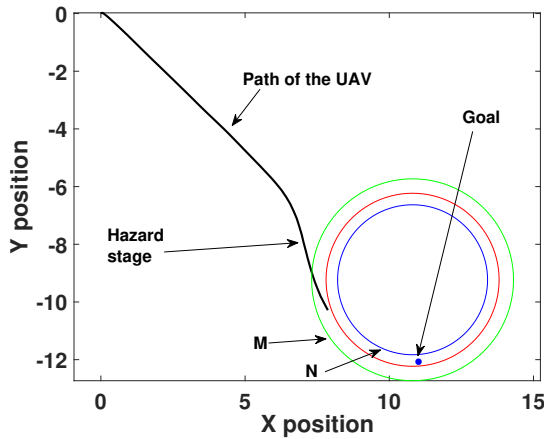


Fig. 14: Hazard stage of the first experiment.

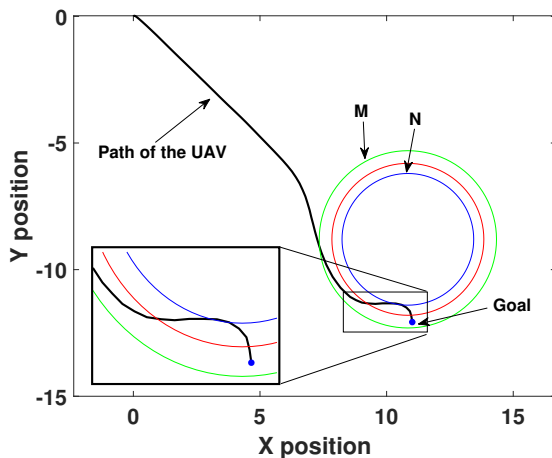


Fig. 15: Intermediate stage of the first experiment.

navigated directly to the goal position (Fig. 16). As indicated in Fig. 16 the hexacopter enters the post hazard stage in an orthogonal direction to the goal. The hexacopter requires a heading correction of $\pi/2 \text{ rad}$ to reach the goal. Due to the dynamics of the UAV the heading correction has been slow towards the goal.

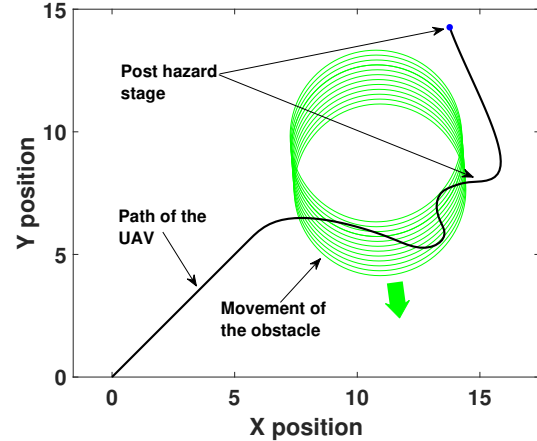


Fig. 16: Paths of the hexacopter and the obstacle in the second experiment.

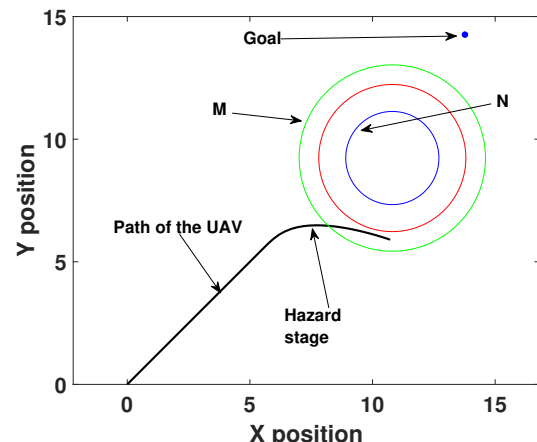


Fig. 17: Hazard stage of the second experiment.

All in all, the experimental and the simulation results strongly confirm the validity of the algorithm proposed.

VI. CONCLUSION AND FUTURE WORK

The paper presents a novel algorithm for time optimal reactive collision avoidance for UAV based navigation applications. The basis of the algorithm is a threefold modified collision cone approach which guarantees the time optimality in single and multiple obstacle scenarios. The time optimality of the proposed method has been proven mathematically. The simulation and the experimental results confirm the validity of the proposed method. As future work the experimental

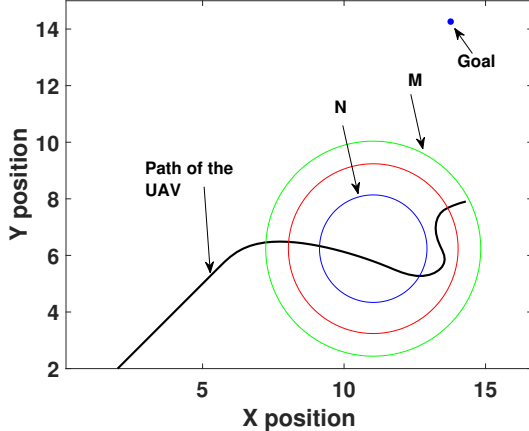


Fig. 18: Intermediate stage of the second experiment.

work would be broadened by incorporating multiple obstacles. Furthermore, instead of the fixed speed assumption made for the UAV, a variable speed and heading avoidance method will be planned.

REFERENCES

- [1] J. A. Steiner, X. He, J. R. Bourne, and K. K. Leang, “Open-sector rapid-reactive collision avoidance: Application in aerial robot navigation through outdoor unstructured environments,” *Robotics and Autonomous Systems*, vol. 112, pp. 211–220, 2019.
- [2] P. E. Hart, N. J. Nilsson, and B. Raphael, “A formal basis for the heuristic determination of minimum cost paths,” *IEEE transactions on Systems Science and Cybernetics*, vol. 4, no. 2, pp. 100–107, 1968.
- [3] A. Stentz, “Optimal and efficient path planning for partially known environments,” in *Intelligent Unmanned Ground Vehicles*. Springer, 1997, pp. 203–220.
- [4] S. Koenig and M. Likhachev, “Fast replanning for navigation in unknown terrain,” *IEEE Transactions on Robotics*, vol. 21, no. 3, pp. 354–363, 2005.
- [5] L. E. Kavraki, P. Svestka, J.-C. Latombe, and M. H. Overmars, “Probabilistic roadmaps for path planning in high-dimensional configuration spaces,” *IEEE transactions on Robotics and Automation*, vol. 12, no. 4, pp. 566–580, 1996.
- [6] S. M. LaValle, “Rapidly-exploring random trees: A new tool for path planning,” 1998.
- [7] O. Khatib, “Real-time obstacle avoidance for manipulators and mobile robots,” in *Proceedings. 1985 IEEE International Conference on Robotics and Automation*, vol. 2. IEEE, 1985, pp. 500–505.
- [8] P. Fiorini and Z. Shiller, “Motion planning in dynamic environments using the relative velocity paradigm,” in *[1993] Proceedings IEEE International Conference on Robotics and Automation*. IEEE, 1993, pp. 560–565.
- [9] Y. Koren, J. Borenstein, et al., “Potential field methods and their inherent limitations for mobile robot navigation.” in *ICRA*, vol. 2, 1991, pp. 1398–1404.
- [10] A. Chakravarthy and D. Ghose, “Obstacle avoidance in a dynamic environment: A collision cone approach,” *IEEE Transactions on Systems, Man, and Cybernetics-Part A: Systems and Humans*, vol. 28, no. 5, pp. 562–574, 1998.
- [11] S. J. Guy, J. Chhugani, C. Kim, N. Satish, M. Lin, D. Manocha, and P. Dubey, “Clearpath: highly parallel collision avoidance for multi-agent simulation,” in *Proceedings of the 2009 ACM SIGGRAPH/Eurographics Symposium on Computer Animation*, 2009, pp. 177–187.
- [12] Y. Abe and M. Yoshiki, “Collision avoidance method for multiple autonomous mobile agents by implicit cooperation,” in *Proceedings 2001 IEEE/RSJ International Conference on Intelligent Robots and Systems. Expanding the Societal Role of Robotics in the the Next Millennium (Cat. No. 01CH37180)*, vol. 3. IEEE, 2001, pp. 1207–1212.
- [13] D. Wilkie, J. Van Den Berg, and D. Manocha, “Generalized velocity obstacles,” in *2009 IEEE/RSJ International Conference on Intelligent Robots and Systems*. IEEE, 2009, pp. 5573–5578.
- [14] B. Gopalakrishnan, A. K. Singh, and K. M. Krishna, “Time scaled collision cone based trajectory optimization approach for reactive planning in dynamic environments,” in *2014 IEEE/RSJ International Conference on Intelligent Robots and Systems*. IEEE, 2014, pp. 4169–4176.
- [15] A. K. Singh, K. M. Krishna, and S. Saripalli, “Planning trajectories on uneven terrain using optimization and non-linear time scaling techniques,” in *2012 IEEE/RSJ International Conference on Intelligent Robots and Systems*. IEEE, 2012, pp. 3538–3545.
- [16] A. K. Singh and K. M. Krishna, “Reactive collision avoidance for multiple robots by non linear time scaling,” in *52nd IEEE Conference on Decision and Control*. IEEE, 2013, pp. 952–958.